Colloids and Surfaces A: Physicochemical and Engineering Aspects 656 (2023) 130342

Contents lists available at ScienceDirect

Colloids and Surfaces A: Physicochemical and Engineering Aspects

journal homepage: www.elsevier.com/locate/colsurfa

# Wetting of aqueous sodium dodecyl sulfate droplets on polydimethylsiloxane surfaces during evaporation

Xiao-Ye Yang [a], Guo-Hao Li [a], Xianfu Huang [b,c,*], Ying-Song Yu [a,**]

[a] Department of Mechanics, School of Civil Engineering, Architecture and Environment, Hubei University of Technology, Wuhan 430068, PR China
[b] State Key Laboratory of Nonlinear Mechanics, Institute of Mechanics, Chinese Academy of Sciences, Beijing 100190, PR China
[c] School of Engineering Science, University of Chinese Academy of Sciences, Beijing 100049, PR China

## GRAPHICAL ABSTRACT

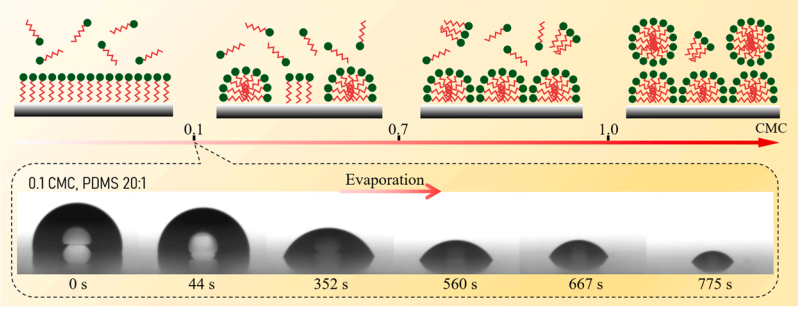


## ARTICLE INFO

*Keywords:*
Droplet
Sodium dodecyl sulfate
Evaporation
Polydimethylsiloxane
Adsorption

## ABSTRACT

Wetting of aqueous sodium dodecyl sulfate (SDS) droplets on polydimethylsiloxane (PDMS) surfaces during evaporation were experimentally studied. After a short-time spontaneous spreading, sessile droplets experienced a period of the constant contact radius (CCR) stage. And it was found that substrate elasticity was found to have an influence on the duration of the CCR stage during the evaporation of aqueous SDS droplets on PDMS surfaces. Moreover, a local contact angle minimum was found during the evaporation of aqueous SDS droplets with an initial SDS concentration below 0.5 CMC. A physical mechanism taking into account the structure of SDS molecules adsorbed at PDMS surfaces was developed for the occurrence of the CCR stage and the local contact angle minimum. Furthermore, two-third power of the instantaneous droplet volume nearly varies linearly with time for all cases.

## 1. Introduction

Evaporation of sessile droplets has found great applications in fields such as pesticide spraying, ink-jet printing, heat transfer and micro-/nanofluidics [1–3]. In 1977, Picknett and Bexon [4] first proposed three evaporation modes of sessile droplets, viz., the constant contact area mode (which is also called the constant contact radius mode, CCR mode), the constant contact angle mode (CCA mode) and the mixed

* Corresponding author at: State Key Laboratory of Nonlinear Mechanics, Institute of Mechanics, Chinese Academy of Sciences, Beijing 100190, PR China.
** Corresponding author.
*E-mail addresses:* huangxf@imech.ac.cn (X. Huang), yuys@hbut.edu.cn (Y.-S. Yu).

https://doi.org/10.1016/j.colsurfa.2022.130342
Received 24 May 2022; Received in revised form 1 October 2022; Accepted 9 October 2022
Available online 14 October 2022

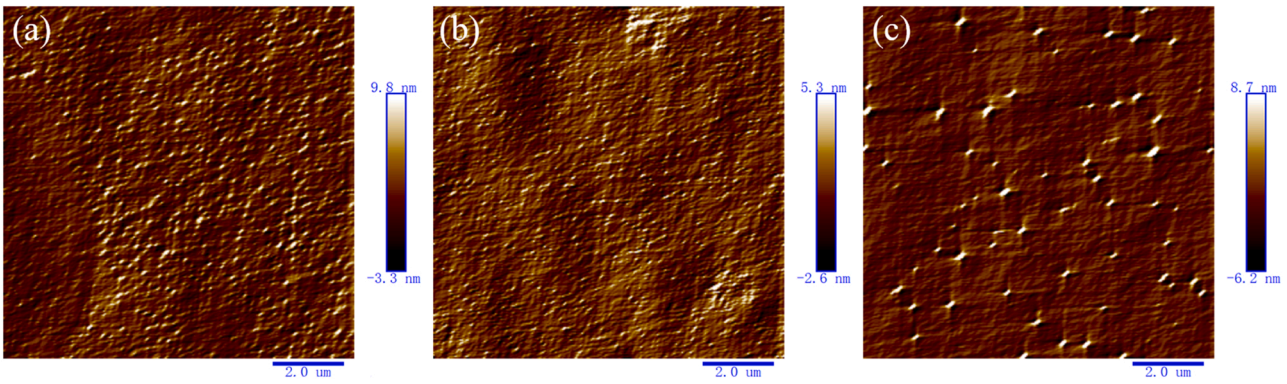


**Fig. 1.** AFM images of PDMS surfaces. (a) PDMS 5:1, (b) PDMS 10:1, (c) PDMS 20:1.

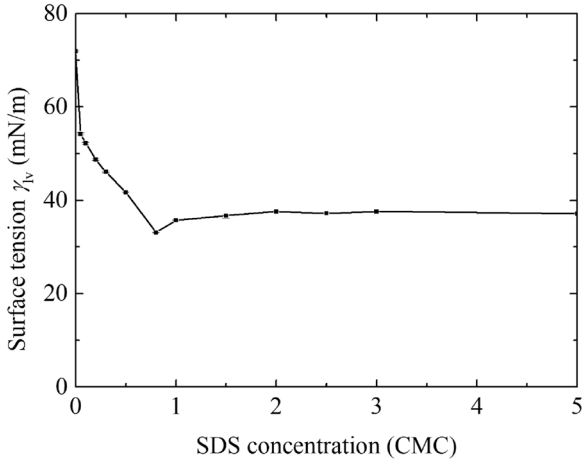


**Fig. 2.** Surface tension of aqueous SDS solutions.

**Table 1**
Wettability of aqueous SDS droplets on PDMS surfaces.

| $c^i_{SDS}$ (CMC) | $\theta_e$ | | | $\theta_r$ | | |
|---|---|---|---|---|---|---|
| | PDMS 5:1 | PDMS 10:1 | PDMS 20:1 | PDMS 5:1 | PDMS 10:1 | PDMS 20:1 |
| 0 | 110° ± 1° | 108° ± 1° | 109° ± 1° | 99° ± 2° | 101° ± 1° | 89° ± 4° |
| 0.05 | 107° ± 1° | 105° ± 1° | 107° ± 1° | 83° ± 1° | 87° ± 2° | 76° ± 1° |
| 0.1 | 102° ± 2° | 102° ± 1° | 104° ± 1° | 75° ± 2° | 78° ± 3° | 76° ± 2° |
| 0.2 | 95° ± 1° | 97° ± 1° | 100° ± 1° | 74° ± 1° | 74° ± 2° | 73° ± 1° |
| 0.3 | 89° ± 2° | 90° ± 2° | 96° ± 1° | 68° ± 2° | 67° ± 2° | 64° ± 1° |
| 0.5 | 78° ± 1° | 79° ± 1° | 79° ± 1° | 62° ± 2° | 63° ± 2° | 57° ± 2° |
| 0.8 | 77° ± 2° | 78° ± 1° | 80° ± 1° | 62° ± 2° | 64° ± 2° | 60° ± 2° |
| 1.0 | 78° ± 1° | 80° ± 1° | 81° ± 1° | 61° ± 2° | 65° ± 2° | 62° ± 1° |

evaporation mode. Evaporation of sessile droplets can be influenced by various factors including the physical and chemical properties of liquid [5–10], surface roughness of the solid substrate [5,6,11–16], surface wettability [12,17], thermal conductivity of the solid substrate [18], substrate elasticity [19–25], substrate temperature [26–28], the inclination of the surface [29–32], application of external fields [33–35], introduction of particles into the liquid [36,37] as well as evaporation environment [38,39].

Surfactants consisting of a polar hydrophilic head and one or more hydrophobic tails have been widely used in industries such as food processing, agriculture, pharmaceutical, and inkjet printing. The introduction of surfactants into a liquid such as water can greatly reduce the surface tension of the liquid. Due to the adsorption of surfactants at the liquid-vapor interface and/or the solid-liquid interface, surfactant-laden droplets will not only easily spread on solid surfaces [40–42], but also have different evaporation characteristics compared to pure liquid droplets [43–48]. Moreover, due to solvent evaporation, the actual SDS concentration will gradually increase and contact line pinning will influence the evaporation. Therefore, understanding the influence of the SDS concentration on the evaporation of aqueous SDS droplets is an important issue.

Polydimethylsiloxane (PDMS) has been widely used in micro/nanofluidics, microelectromechanical systems and lab-on-a-chip devices, etc. And variations in the wettability during the evaporation of a liquid may influence the performance of these devices. Adding surfactants to the liquid may help to improve the performance. Under the action of the vertical component of liquid-vapor interfacial tension, PDMS surface will be deformed by a sessile droplet [49–52]. This deformation can also make a sessile droplet experiencing a longer CCR stage [19–25]. When there is a sessile droplet containing surfactants on PDMS surfaces, the surface deformation induced by the vertical component of the reduced liquid-vapor interfacial tension will be much smaller. In this case, does substrate elasticity still have a significant influence on the evaporation of surfactant-laden droplets?

In this paper, wetting of sessile aqueous SDS droplets on PDMS surfaces during evaporation are experimentally investigated. It is found that with the addition of SDS molecules, both the apparent and receding contact angles greatly decrease with increasing SDS concentration below 0.5 critical micelle concentration (CMC, 8.2 mM [47]) and nearly keep unchanged in the concentration range from 0.5 CMC to 1.0 CMC. On PDMS surfaces, a short period of spontaneous spreading is observed at the early stage of the evaporation when SDS molecules are introduced into the liquid. Moreover, the evaporation characteristics of aqueous SDS droplets on the PDMS surfaces strongly depends on the initial SDS concentration, which could be attributed to the relationship of the receding contact angle with instantaneous SDS concentration. In addition, two-third power of instantaneous droplet volume was analyzed and it was found that both initial SDS concentraion and substrate elasticity had no obvious influence on evaporation rate.

## 2. Materials and methods

PDMS with the mass ratios of base (Dowsil™ 184 silicone elastomer base, Dow Europe GMHB C/O Dow Silicones Deutschland GMBH) to curing agent (Dowsil™ 184 silicone elastomer curing agent, Dow Europe GMHB C/O Dow Silicones Deutschland GMBH) of 5:1, 10:1 and 20:1 was prepared using the spin-coating method. Surface roughness of these

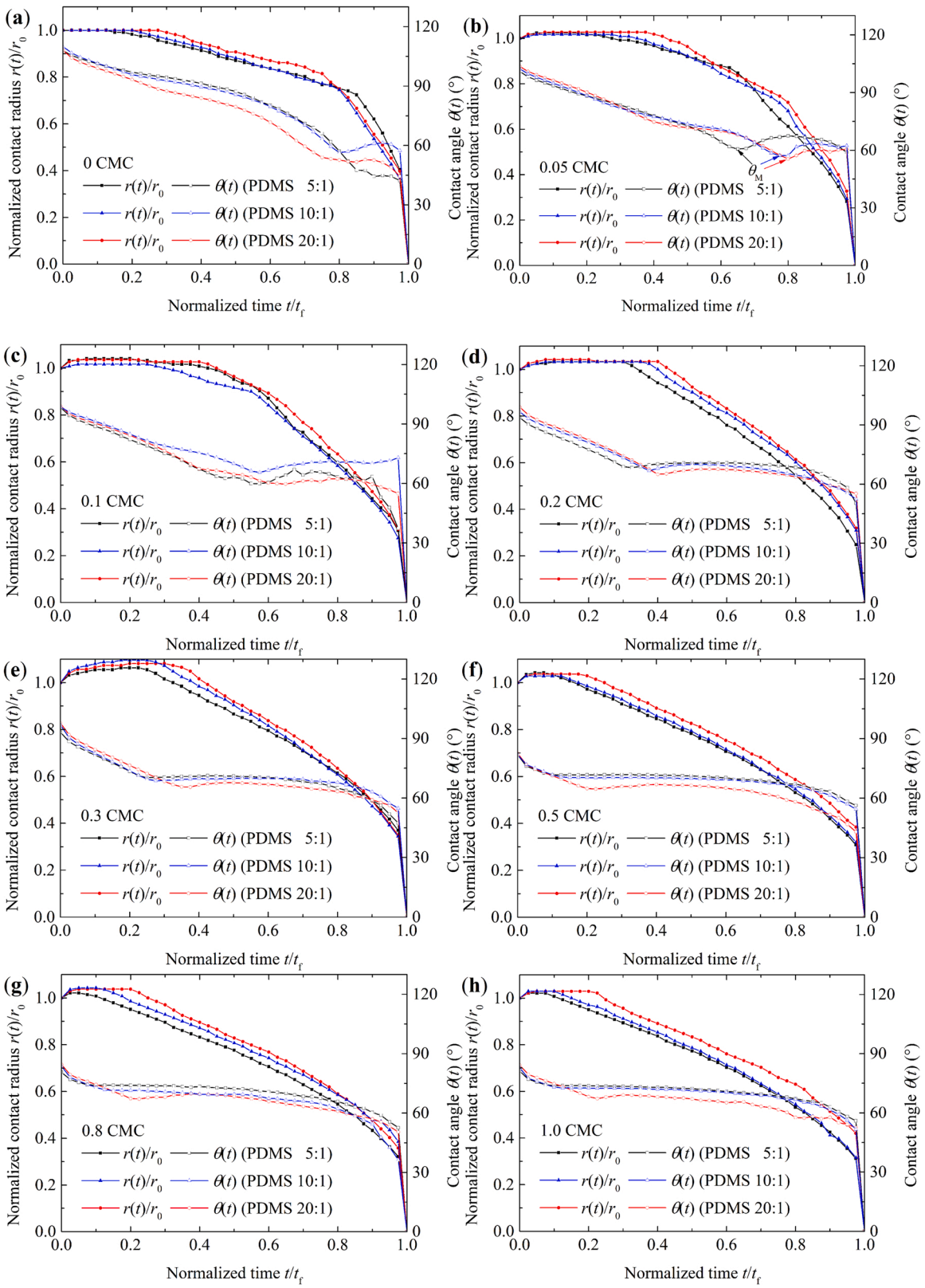


**Fig. 3.** Evaporation curves of aqueous SDS droplets with different initial SDS concentrations on PDMS surfaces. (a) 0 CMC, (b) 0.05 CMC, (c) 0.1 CMC, (d) 0.2 CMC, (e) 0.3 CMC, (f) 0.5 CMC, (g) 0.8 CMC and (h) 1.0 CMC.

PDMS surfaces was characterized using an atomic force microscopy (AFM, Dimension Icon, Bruker, USA) by randomly scanning a region of 10 μm× 10 μm, as shown in Fig. 1. The values of root-mean-square roughness of these surfaces were, respectively, 2.4 nm, 1.6 nm and 3.1 nm, indicating that these PDMS surfaces could be regarded as smooth.

SDS with a purity of ≥ 99 % (Sigma-Aldrich) was dissolved in deionized water to obtain SDS solutions with concentrations of 0.05, 0.1,

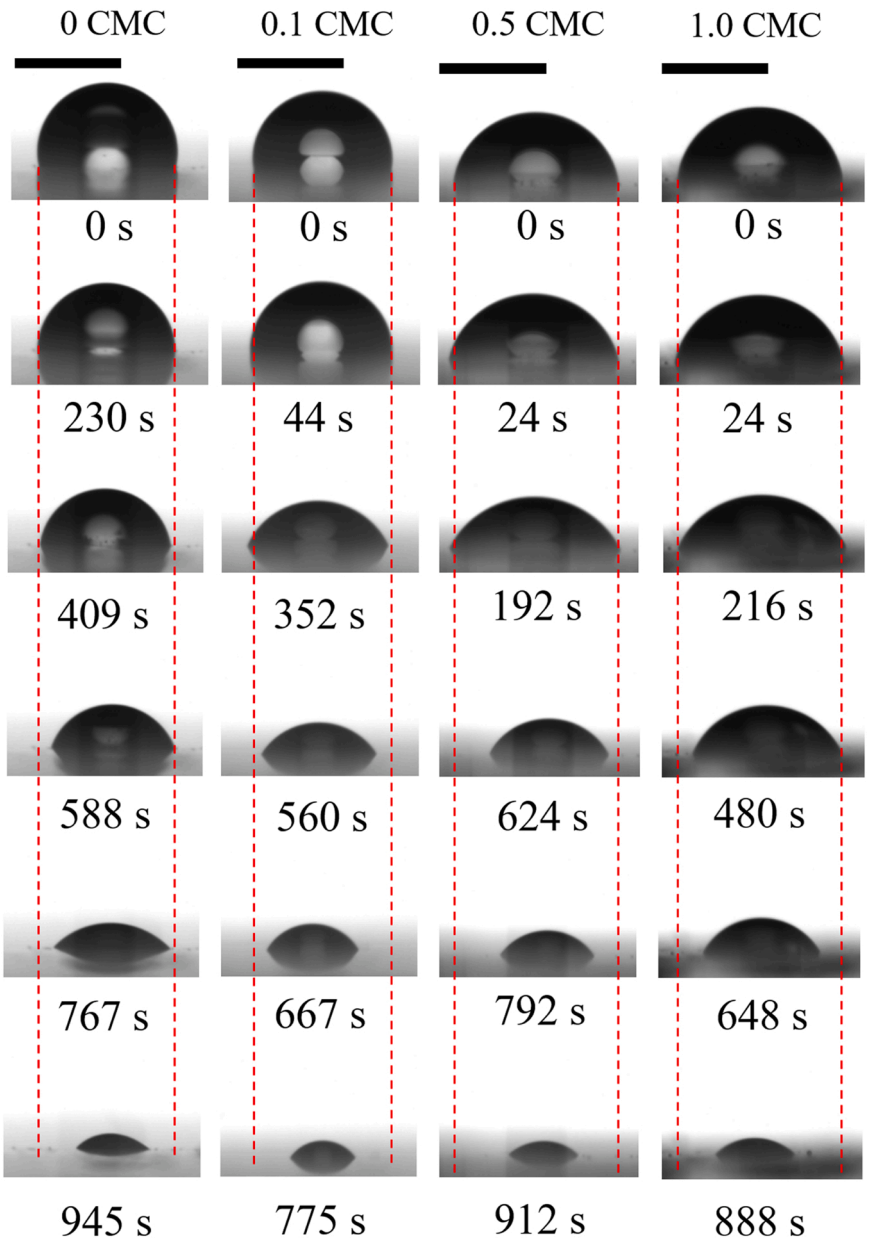


**Fig. 4.** Snapshots of evaporating aqueous SDS droplets on PDMS 20:1. All inserted scale bars represent 1 mm.

0.2, 0.3, 0.5, 0.8 and 1.0 CMC. All solutions were prepared in glass and plastic containers which have been cleaned in advance with acetone, ethanol and deionized water consecutively. Each solution was used within a day from its preparation.

The surface tension of aqueous SDS solutions was measured using a dynamic contact angle measuring devices and tensiometer (DCAT11, Dataphysics, Germany). Before measurement, both sample vessels and a Wilhelmy plate (PT 11, width: 19.9 mm, thickness: 0.2 mm) made of platinum-iridium was ultrasonically stirred in deionized water, ethanol and acetone successively. Then the plate was made red-hot in a gas flame to ensure that it is clean and was inserted in the DCAT11 later. Appropriate volume of an aqueous SDS solution was poured into the clean sample vessel, which was later placed in the hole of the stage. The sample vessel with the liquid was moved up until a weight difference can be detected by the balance. The speed of the lift motor was set at 1.00 mm/s for detecting the surface of the liquid. The surface detectiong threshold value and the immersion depth were set at 8.00 mg and 3.00 mm, respectivley. Five measurements were made within one second. The measurement will be stopped if the standard deviation of the surface tension is smaller than 0.03 mN/m over the last 50 measurement cycles. After setting the above parameters and pressing “start”, the value of surface tension of the aqueous SDS solution will be obtained automatically. The ambient temperature and relative humidity for measuring the surface tension of aqueous SDS solutions were 23 ± 1 ℃ and 39 ± 2 %, respectively. Each experiment was repeated three times to ensure the reproducibility.

The static apparent contact angle was measured from the image of an aqueous SDS droplet with a nominal volume of 1.0 μL on a PDMS surface. As aqueous SDS droplets could spontaneously spread on PDMS surfaces when gently deposited, the advancing contact angle was not measured and the receding contact angle of aqueous SDS droplets on the PDMS surfaces were measured by retracting liquid from the droplet using a DSA 30 droplet shape analyzer (Krüss, Germany) following the procedure suggested by Huhtamäki et al. [53]. First, an aqueous SDS droplet with a nominal volume of 35 μL was deposited onto a PDMS surface. Then the height of the stage was adjusted to ensure the needle

**Table 2**
Values of the instantaneous bulk SDS concentration at the beginning and end of the CCR stage.

| $c^i_{SDS}$ (CMC) | $c_1$ (CMC) | | | $c_2$ (CMC) | | |
|---|---|---|---|---|---|---|
| | PDMS 5:1 | PDMS 10:1 | PDMS 20:1 | PDMS 5:1 | PDMS 10:1 | PDMS 20:1 |
| 0.05 | 0.054 ± 0.003 | 0.054 ± 0.003 | 0.055 ± 0.003 | 0.066 ± 0.005 | 0.079 ± 0.005 | 0.084 ± 0.004 |
| 0.1 | 0.104 ± 0.004 | 0.103 ± 0.003 | 0.104 ± 0.004 | 0.151 ± 0.006 | 0.157 ± 0.007 | 0.206 ± 0.007 |
| 0.2 | 0.215 ± 0.005 | 0.215 ± 0.006 | 0.215 ± 0.005 | 0.338 ± 0.008 | 0.391 ± 0.009 | 0.422 ± 0.008 |
| 0.3 | 0.334 ± 0.008 | 0.362 ± 0.011 | 0.362 ± 0.009 | 0.456 ± 0.014 | 0.462 ± 0.013 | 0.523 ± 0.012 |
| 0.5 | 0.520 ± 0.007 | 0.519 ± 0.013 | 0.520 ± 0.010 | 0.584 ± 0.016 | 0.602 ± 0.015 | 0.693 ± 0.015 |
| 0.8 | 0.830 ± 0.008 | 0.812 ± 0.011 | 0.831 ± 0.009 | 0.892 ± 0.017 | 0.948 ± 0.018 | 1.094 ± 0.017 |
| 1.0 | 1.034 ± 0.008 | 1.037 ± 0.012 | 1.037 ± 0.011 | 1.120 ± 0.019 | 1.168 ± 0.016 | 1.433 ± 0.018 |

**Table 3**
Values of the local contact angle minimum and the bulk SDS concentration at the local contact angle minimum.

| $c^i_{SDS}$ (CMC) | $\theta_M$ | | | $c(\theta_M)$ (CMC) | | |
|---|---|---|---|---|---|---|
| | PDMS 5:1 | PDMS 10:1 | PDMS 20:1 | PDMS 5:1 | PDMS 10:1 | PDMS 20:1 |
| 0.05 | 59° ± 1° | 59° ± 1° | 56° ± 1° | 0.17 ± 0.02 | 0.19 ± 0.02 | 0.21 ± 0.04 |
| 0.1 | 59° ± 1° | 66° ± 1° | 59° ± 1° | 0.33 ± 0.02 | 0.34 ± 0.01 | 0.43 ± 0.03 |
| 0.2 | 70° ± 2° | 68° ± 1° | 64° ± 1° | 0.36 ± 0.03 | 0.41 ± 0.02 | 0.42 ± 0.02 |
| 0.3 | 68° ± 1° | 67° ± 1° | 65° ± 1° | 0.48 ± 0.02 | 0.47 ± 0.01 | 0.56 ± 0.02 |
| 0.5 | 71° ± 2° | 69° ± 2° | 63° ± 1° | 0.76 ± 0.02 | 0.70 ± 0.02 | 0.75 ± 0.02 |

was close to the sample surface without any contact and liquid was removed from the drop at 2 μL/s until the volume was about 13 μL (the position of the needle was adjusted again if needed). Consequently, 2 μL was removed at 0.05 μL/s to avoid dynamic effects. After 30 s′ waiting, the liquid was withdrawed at 0.05 μL/s for the determination of the receding contact angle until the droplet was completely removed. The receding contact angle was measured from the images during the retraction of the droplet and its value was an average of five measurements. Each experiment was repeated three times to ensure the result is reproducible.

The evaporation of SDS droplets with a nominal volume of 0.80 μL on these surfaces was recorded using the DSA 30 droplet shape analyzer at 1 fps (frame per second). Each experiment was conducted three times to ensure the reproducibility. The experiments of both the surface wettability and the evaporation of aqueous SDS droplets PDMS surfaces were conducted in a room with the door and the window closed. The ambient temperature and relative humidity were monitored using a thermo-hygrometer and the corresponding values were 26 ± 1 ℃ and 39 ± 2 %, respectively.

## 3. Results and discussion

### 3.1. Wettability of aqueous SDS droplets on PDMS surfaces

Fig. 2 shows the surface tension of aqueous SDS solutions with different concentrations. The surface tension of an aqueous SDS solution decreased with increasing SDS concentration, with a minimum of 33.1 mN/m at 0.8 CMC. Then it slowly increased to 35.7 mN/m at 1.0 CMC. Above 1 CMC, the surface tension was found to remain almost constant. The experimental results are consistent with the results in Refs. [54–56]. The concentration of an aquesous SDS solution for the minimum of surface tension of aqueous SDS droplets was found to be less than 1 CMC, which seems exceptional. This could be attributed to the presence of minor amounts of an impurity (SDS was used without further extraction), which increases the adsorption of SDS molecules [54].

Table 1 lists the values of the apparent and receding contact angles of aqueous SDS droplets on planar PDMS surfaces, denoted by $\theta_e$ and $\theta_r$, respectively (the values of apparent and receding contact angles above 1.0 CMC were not given because in this case the adsorption of SDS molecules at the solid-liquid and liquid-vapor interfaces gets saturated). Values of the advancing contact angle were not given because aqueous SDS droplets will spontaneously spread for a short time after they are gently deposited on PDMS surfaces. For all surfaces, the values of $\theta_e$ and $\theta_r$ decreased with increasing SDS concentration when SDS concentration is below 0.5 CMC. With further addition of SDS molecules, both $\theta_e$ and $\theta_r$ nearly remained unchanged. At a low SDS concentration (<0.1 CMC), the receding contact angle for aqueous SDS droplets on PDMS 20:1 was much less than that on PDMS 5:1 and PDMS 10:1, which could be attributed to the surface deformation induced by vertical component of liquid-vapor interfacial tension. However, with further addition of SDS molecules, there is only a slight or neglible influence of substrate

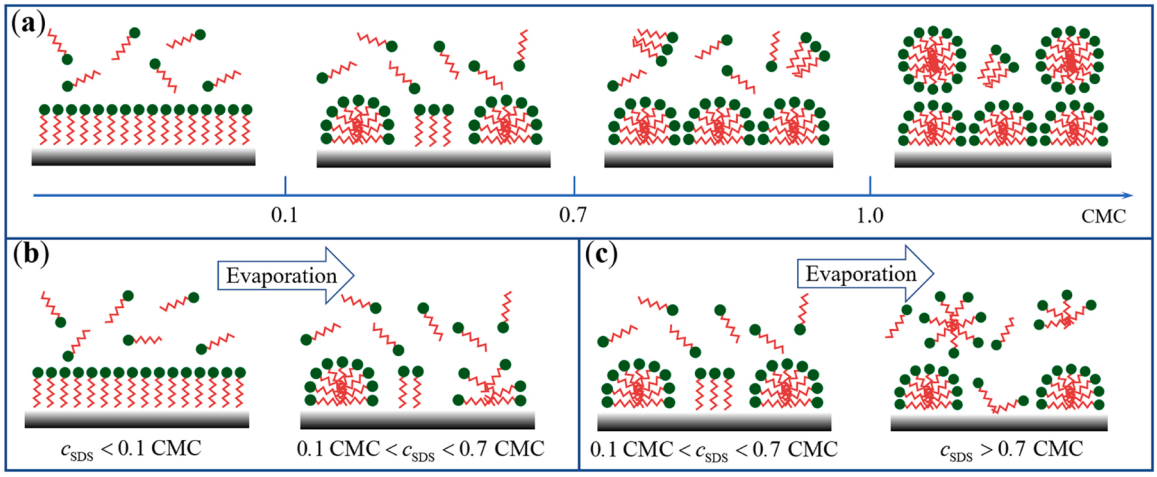


**Fig. 5.** (a) Schematics of the structure of adsorpted SDS molecules on PDMS surfaces based on the works of Kwieciński et al. [47] and Duan et al. [58]. (b) Formation of disordered SDS aggregate during the evaporation of aqueous SDS droplets with initial concentrations less than 0.1 CMC and (c) that for initial concentrations ranging from 0.1 CMC to 0.7 CMC.

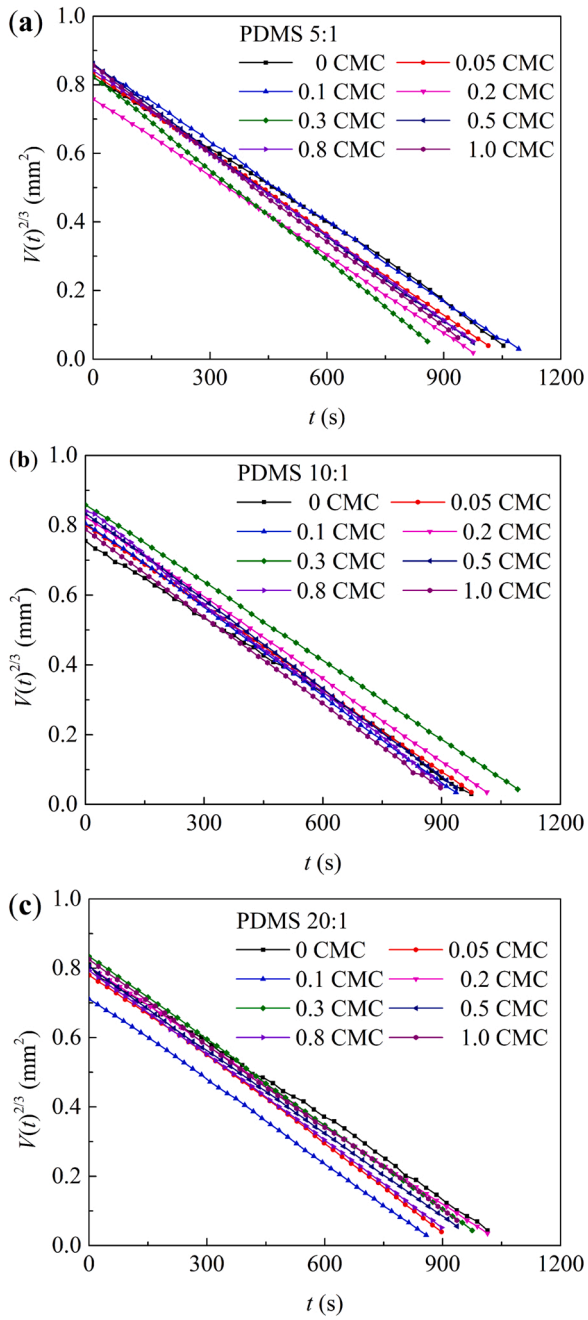


**Fig. 6.** Influence of initial SDS concentration on evaporation rate of aqueous SDS droplets with different initial SDS concentrations on PDMS surfaces. (a) PDMS 5:1, (b) PDMS 10:1, (c) PDMS 20:1.

elasticity on the receding contact angle.

### 3.2. Evaporation of aqueous SDS droplets on PDMS surfaces

Fig. 3 shows the evolution of normalized contact radius (ratio of the instantaneous contact radius to the initial contact radius) and contact angle of evaporating aqueous SDS droplets with initial SDS concentrations ranging from 0 to 1.0 CMC on PDMS surfaces versus normalized time $t/t_f$, where $t_f$ denotes the whole evaporation time. For pure water droplets, the evaporation started first with the CCR mode. And the softer the substrate, the longer the CCR stage (see Fig. 3(a)), which can be attributed to the surface deformation due to the action of the vertical component of liquid-vapor interfacial tension [19–25]. For aqueous SDS droplets, similar phenomena were also found, as shown in Fig. 3(b)-(h). However, the evaporation of aqueous SDS-laden droplets behaved differently depending on the initial SDS concentration. The contact line of all aqueous SDS droplets advanced spontaneously for a short period on all PDMS surfaces regardless of the initial concentration. Such a short-time spontaneous spreading can be attributed to the change of the wetting characteristics at the contact line because SDS molecules are transferred from the droplet onto PDMS surfaces [57]. After the short-time spreading, the evaporation of aqueous SDS droplets followed different processes depending on the initial SDS concentration. At a low SDS concentration of 0.05 CMC (Fig. 3b), a mixed evaporation mode followed the CCR stage until local minimum values of contact angle $\theta_M = 59^\circ$, $59^\circ$ and $56^\circ$ for the droplets evaporating on PDMS 5:1, PDMS 10:1 and PDMS 20:1 were reached, respectively. Then the contact angle increased gradually until a local contact angle maximum is reached. From this instant, the evaporation switched to the CCA mode and finally ended with mixed mode. Similar phenomena were also found in the evaporation of aqueous SDS droplets with an initial SDS concentration of 0.1 CMC on PDMS surfaces except that there was no obvious increase in the contact angle after the contact angle minimum for the droplet evaporating on PDMS 20:1 was reached.

For aqueous SDS droplets with an initial SDS concentration ranging from 0.2 CMC to 1.0 CMC, the droplets evaporated in the CCR mode after a short-time spontaneous spreading, then the evaporation switched to the CCA stage and finally ended with the mixed mode, as shown in Fig. 3(c)-(h). Moreover, a local contact angle minimum was also observed from each of the evaporation curves though it was not obvious. From Fig. 2, it was found that it would take more time for the droplet with a lower initial SDS concentration having the local contact angle minimum, which was also found in the experiments by Kwieciński et al. [47]. In case of the evaporation of pure water droplets [19–25], it was found that the softer the substrate, the longer the strong CCR stage. Though the addition of SDS molecules gradually reduce the surface tension of the liquid, there is still obvious influence of substrate elasticity on the duration of the contact line pinning stage. Besides, as shown in Fig. 3, the occurrence of the CCA stage was found to be earlier with the increase of the initial SDS concentration (no more than 0.5 CMC). As an example, Fig. 4 shows the time-varying images extracted from the videos of evaporating aqueous SDS droplets on PDMS 20:1.

Table 2 lists the values of the instantaneous bulk SDS concentration when the CCR stage started and ended, denoted as $c_1$ and $c_2$, respectively. It was found $c_1$ was nearly independent on substrate elasticity. However, the softer the substrate, the higher the instantaneous bulk SDS concentration, which could be attributed to the deformation of PDMS surfaces due to the vertical component of liquid-vapor interfacial tension [1,20,21]. Under the action of vertical component of liquid-vapor interfacial tension, a PDMS surface will be deformed with an elastic stored energy per unit length of the contact line of the order of $\gamma_{lv}{}^2\sin^2\theta(1-\nu^2)/E$ [20,21], where $E$ and $\nu$ are Young's modulus and Possion's ratio of the PDMS surface. For aqueous SDS droplets with the same initial SDS concentration, there was only a slight difference in the instantaneous contact angle during the CCR stage. As reported in Ref. [21], a PDMS surface with a higher mass ratio of base to curing agent has a lower Young's modulus. Thus, there would be more elastic energy stored in the softer PDMS film. Such an energy acts as a barrier to prevent the contact line from depinning and therefore a longer CCR stage would be observed during the evaporation of aqueous SDS droplets on a softer PDMS surface. Besides, the liquid-vapor interfacial tension and contact angle are greatly dependent on SDS concentration, as shown in Fig. 2 and Table 1, respectively. As a result, the duration of the CCR stage was found to be different if the initial SDS concentration is varied, as shown in Fig. 3.

Table 3 lists the values of the contact angle minimum and the bulk SDS concentration at the local contact angle minimum. On PDMS 5:1, the local contact angle minimum kept unchanged for aqueous SDS droplets with an initial SDS concentration of 0.05 or 0.1 CMC. With

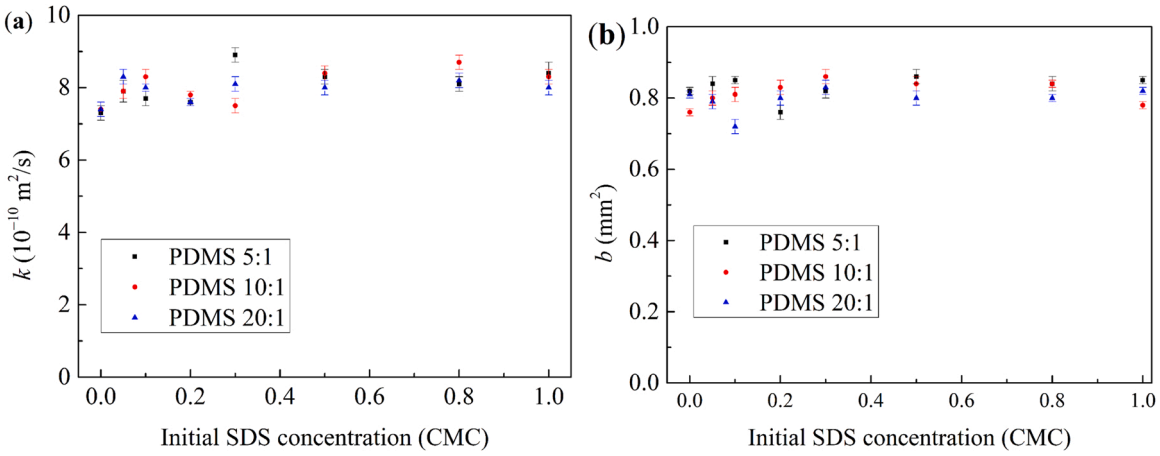


**Fig. 7.** Values of fitting parameters $k$ and $b$.

further addition of SDS molecules, the local minimum increased sharply and there was no obvious change in the minimum. On PDMS 10:1, the local minimum has a minimum at the initial SDS concentration of 0.05 CMC and it varied slightly at an initial SDS concentration above 0.1 CMC. On PDMS 20:1, there was a minimum of the local contact angle minimum at an initial SDS concentration. Then it slightly increased with increasing initial SDS concention and kept nearly unchanged at an initial SDS concentration above 0.2 CMC. As reported in Ref. [47], the local minimum might depend on the instantaneous SDS concentration in the droplets. From Table 3, it is easily found that at low initial SDS concentrations (<0.1 CMC), the local contact angle minimum is smaller than the corresponding static receding contact angle, however, the minimum is slightly greater than the static receding contact angle above 0.1 CMC.

The physical mechanism by which contact line pinning occurs is that the structure of SDS molecules adsorbed on the PDMS surface depends on the initial concentration of the SDS droplets (Fig. 5(a)) [47,58]. For evaporative SDS droplets with an initial concentration < 0.1 CMC, SDS molecules mainly formed an amorphous layer on the PDMS surface [58]. The SDS concentration gradually increased with the evaporation of water. When the concentration reaches a threshold, dome-shaped half-micelles may form on the substrate. The transition from the amorphous layer to the dome-like half-micelle requires energy, and the pre-absorbed amorphous layer hinders the formation of the dome-shaped half-micelles. Consequently, disordered surface aggregates are also formed simultaneously (Fig. 5(b)), which have non-uniform wetting properties, resulting in the pinning of contact lines [58]. With a further increase in the instantaneous SDS concentration, the disordered SDS layer is reorganized into a homogeneous layer, giving the surface the same surface wetting properties, leading to a smooth local retraction of the contact line and a minimal local contact angle [47]. For sessile droplets with initial SDS concentrations in the range from 0.1 to 0.7 CMC, only part of the wetted PDMS surface was covered by an amorphous layer (Fig. 5(c)). Consequently, the duration of the CCR phase becomes shorter (see Fig. 3), and the local contact angle minimum is larger than that of droplets with initial concentrations less than 0.1 CMC [58].

### 3.3. Instantaneous volume of aqueous SDS droplets

To find the effect of initial SDS concentration on the evaporation characteristics of aqueous SDS droplets on PDMS surfaces, the evolution of two-third power of the instantaneous droplet volume $V(t)$ versus time $t$ was plotted, as shown in Fig. 6. From Fig. 6, on each surface, the two-third power of instantaneous droplet volume varied linearly with time as $V(t)^{2/3} = -kt + b$ [4,59], where $k$ and $b$ are fitting parameters. Using the least square method, the values of $k$ and $b$ were obtained, as shown in Fig. 7. For a pure water droplet, the parameter $k$ nearly kept unchanged regardless of the mass ratio of PDMS surfaces. With the addition of SDS molecules, it had a slight increase because the liquid-vapor interfacial tension is reduced, resulting in a larger liquid-air interfacial area. For most cases, there was only slight difference in the parameter $k$ except for the droplets with an initial SDS concentration of 0.3 CMC. In conclusion, two-third power of instantaneous volume of evaporating sessile aqueous SDS droplets varies linearly with time independent of substrate elasticity and initial SDS concentration. Strickly speaking, for an isothermal diffusion-controlled evaporation of a sessile droplet, the instantaneous droplet volume obeys a two-third power law at the CCA stage while it follows different power laws at the CCR stage depending on the contact angle [59]. However, there might be strong flows such as capillary flow and Marangoni flow and a complex droplet temperature due to the loss of solvent [4]. Besides, air flow may also influence the evaporation of sessile droplets, especially in an open environment [4]. Therefore, it is still a big challenge to quantitatively elucidate why the instantaneous volume of evaporating sessile droplets with a relatively high evaporation property follow a certain power law from thermodynamics.

## 4. Conclusion

Evaporation of aqueous SDS droplets on PDMS surfaces with base-to-curing agent mass ratios of 5:1, 10:1 and 20:1 was experimentally investigated. Because of the transfer of SDS molecules from the droplet to PDMS surfaces, the evaporation started with a short-time spontaneous spreading. Then it switched to the CCR stage. Under the action of vertical component of liquid-vapor interfacial tension, PDMS films will be deformed and the elastic stored energy acts as a barrier to hinder the receding of the contact line. Meanwhile, surface tension of aqueous SDS solution is greatly dependent on SDS concentration. Thus, both substrate elasticity and SDS concentration were found to have an influence on the duration of the CCR stage. Moreover, there existed a local contact angle minimum during the evaporation of aqueous SDS droplets with an initial SDS concentration no more than 0.5 CMC. Both the occurrence of the CCR stage and the local contact angle minimum could be attributed to the structure of SDS molecules absorbed at PDMS surfaces. Besides, two-third power of instantaneous droplet volume was found to nearly vary linearly with time for all cases independent of SDS concentration and substrate elasticity. The present work highlights the wettability and evaporation of surfactant-laden droplets on soft substrates and the influence of substrate elasticity and surfactant concentration on evaporation characteristics.

## CRediT authorship contribution statement

**Xiaoye Yang**: Conceptualization, Methodology, Investigation, Writing – original draft. **Guohao Li**: Conceptualization, Methodology, Investigation, Writing – original draft. **Xianfu Huang**: Conceptualization, Methodology, Writing – review & editing, Project administration, Funding acquisition. **Yingsong Yu**: Conceptualization, Methodology, Writing – review & editing, Supervision, Project administration, Funding acquisition.

## Declaration of Competing Interest

There are no conflicts of interest to declare.

## Acknowledgments

This work was jointly supported by the National Natural Science Foundation of China (Grant No.: 11572114) and the Chinese Academy of Sciences Key Research Program of Frontier Sciences (Grant No.: QYZDJ-SSW-JSC019).

## References

[1] Y.P. Zhao, Physical Mechanics of Surfaces and Interfaces, Science Press, Beijing, 2012.
[2] Y.P. Zhao, Nano and Mesoscopic Mechanics, Science Press, Beijing, 2014.
[3] H.Y. Erbil, Evaporation of pure liquid sessile and spherical suspended drops: a review, Adv. Colloid Interface Sci. 170 (1–2) (2012) 67–86.
[4] R.G. Picknett, R. Bexon, The evaporation of sessile or pendant drops in still air, J. Colloid Interface Sci. 61 (2) (1977) 336–351.
[5] Y.S. Yu, L. Sun, X.F. Huang, J.Z. Zhou, Evaporation of ethanol/water mixture droplets on a pillar-like PDMS surface, Colloid Surf. A 574 (2019) 215–220.
[6] Y.S. Yu, X.F. Huang, L. Sun, J.Z. Zhou, A. Zhou, Evaporation of ethanol/water mixture droplets on micro-patterned PDMS surfaces, Int. J. Heat. Mass Transf. 144 (2019), 118708.
[7] H. Sadafi, R. Rabani, S. Dahaeck, H. Machrafi, B. Haut, P. Dauby, P. Colinet, Evaporation induced demixing in binary sessile drops, Colloid Surf. A 602 (2020), 125052.
[8] Y.X. Li, P.Y. Lv, C. Diddens, H.S. Tan, H. Wijshoff, M. Versluis, D. Lohse, Evaporation-triggered segregation of sessile binary droplets, Phys. Rev. Lett. 120 (22) (2018), 224501.
[9] A.M.J. Edwards, P.S. Atkinson, C.S. Cheung, C.H. Liang, D.J. Fairhurst, F.F. Ouali, Density-driven flows in evaporating binary liquid droplets, Phys. Rev. Lett. 121 (18) (2018), 184501.
[10] T. Ozturk, H.Y. Erbil, Evaporation of water-ethanol binary sessile drop on fluoropolymer surfaces: influence of relative humidity, Colloid Surf. A 553 (2018) 327–336.
[11] D.H. Shin, S.H. Lee, C.K. Choi, S. Retterer, The evaporation and wetting dynamics of sessile water droplets on submicron-scale patterned silicon hydrophobic surfaces, J. Micromech. Micro 20 (5) (2010), 055021.
[12] G. McHale, S. Aqil, N.J. Shirtcliffe, M.I. Newton, H.Y. Erbil, Analysis of droplet evaporation on a superhydrophobic surface, Langmuir 21 (24) (2005) 11053–11060.
[13] X.M. Chen, R.Y. Ma, J.T. Li, C.L. Hao, W. Guo, B.L. Luk, S.C. Li, S.H. Yao, Z. K. Wang, Evaporation of droplets on superhydrophobic surfaces: surface roughness and small droplet size effects, Phys. Rev. Lett. 109 (11) (2012), 116101.
[14] W. Xu, R. Leeladhar, Y.T. Kang, C.H. Choi, Evaporation kinetics of sessile water droplets on micropillared superhydrophobic surfaces, Langmuir 29 (20) (2013) 6032–6041.
[15] F.C. Wang, H.A. Wu, Pinning and depinning mechanism of the contact line during evaporation of nano-droplets sessile on textured surfaces, Soft Matter 9 (24) (2013) 5703–5709.
[16] T. Pham, S. Kumar, Drying of droplets of colloidal suspensions on rough substrates, Langmuir 33 (38) (2017) 10061–10076.
[17] D.H. Shin, S.H. Lee, J.Y. Jung, J.Y. Yoo, Evaporating characteristics of sessile droplet on hydrophobic and hydrophilic surfaces, Microelectron. Eng. 86 (4–6) (2009) 1350–1353.
[18] G.J. Dunn, S.K. Wilson, B.R. Duffy, S. David, K. Sefiane, The strong influence of substrate conductivity on droplet evaporation, J. Fluid Mech. 623 (2009) 329–351.
[19] G. Pu, S.J. Severtson, Water evaporation on highly viscoelastic polymer surfaces, Langmuir 28 (26) (2012) 10007–10014.
[20] M.C. Lopes, E. Bonaccurso, Evaporation control of sessile water drops by soft viscoelastic surfaces, Soft Matter 8 (30) (2012) 7875–7881.
[21] Y.S. Yu, Z.Q. Wang, Y.P. Zhao, Experimental study of evaporation of sessile water droplet on PDMS surfaces, Acta Mech. Sin. 29 (6) (2013) 799–805.
[22] Y.C. Chuang, C.K. Chu, S.Y. Lin, L.J. Chen, Evaporation of water droplets on soft patterned surfaces, Soft Matter 10 (19) (2014) 3394–3403.
[23] J. Gerber, T.M. Schutzius, D. Poulikakos, Patterning of colloidal droplet deposits on soft materials, J. Fluid Mech. 907 (2021) A39.
[24] S. Shyam, P.K. Mondal, B. Mehta, Field driven evaporation kinetics of a sessile ferrofluid droplet on a soft substrate, Soft Matter 16 (28) (2020) 6619–6632.
[25] V. Charitatos, S. Kumar, Droplet evaporation on soft solid substrates, Soft Matter 17 (41) (2021) 9339–9352.
[26] F. Girard, M. Antoni, S. Faure, A. Steinchen, Influence of heating temperature and relative humidity in the evaporation of pinned droplets, Colloid Surf. A 323 (1–3) (2008) 36–49.
[27] J.J. Zhang, H.B. Huang, X.Y. Lu, Pinning-depinning mechanism of the contact line during evaporation of nanodroplets on heated heterogeneous surfaces: a molecular dynamics simulation, Langmuir 35 (19) (2019) 6356–6366.
[28] Y. Liu, M. Monde, Y. Mitsutake, K. Tsubaki, Evaporation time and vapor generation limit of a droplet on a hot surface, Int. J. Heat. Mass Transf. 173 (2021), 121280.
[29] M. Gopu, S. Rathod, U. Namangalam, R.K. Pujala, S.S. Kumar, D. Mampallil, Evaporation of inclined drops: formation of asymmetric ring patterns, Langmuir 36 (28) (2020) 8137–8143.
[30] M.L. Timm, E. Dehdashti, A.J. Darban, H. Masoud, Evaporation of a sessile droplet on a slope, Sci. Rep. 9 (2019) 19803.
[31] J.Y. Kim, I.G. Hwang, B.M. Weon, Evaporation of inclined water droplets, Sci. Rep. 7 (2017) 42848.
[32] V. Charitatos, T. Pham, S. Kumar, Droplet evaporation on inclined substrates, Phys. Rev. Fluids 6 (8) (2021), 084001.
[33] H. Almohammadi, A. Amirfazli, Sessile drop evaporation under an electric field, Colloid Surf. A 555 (2018) 580–585.
[34] S. Shyam, P.K. Mondal, B. Mehta, Field driven evaporation kinetics of a sessile ferrofluid droplet on a soft substrate, Soft Matter 16 (28) (2020) 6619–6632.
[35] M.J. Gibbons, A.I. Garivalis, S. O'Shaughnessy, P. di Marco, A.J. Robinson, Evaporating hydrophilic and superhydrophobic droplets in electric fields, Int. J. Heat. Mass Transf. 164 (2021), 120539.
[36] D. Orejon, K. Sefiane, M.E.R. Shanahan, Stick-slip of evaporating droplets: substrate hydrophobicity and nanoparticle concentration, Langmuir 27 (21) (2011) 12834–12843.
[37] Y.H. Chen, A. Askounis, V. Koutsos, P. Valluri, Y. Takata, S.K. Wilson, K. Sefiane, On the effect of substrate viscoelasticity on the evaporation kinetics and deposition patterns of nano-suspension drops, Langmuir 36 (1) (2020) 204–213.
[38] M.A. Kazemi, D.S. Nobes, J.A.W. Elliott, Experimental and numerical study of the evaporation of water at low pressures, Langmuir 33 (18) (2017) 4578–4591.
[39] S. Radhakrishnan, T.N.C. Anand, S. Bakshi, Evaporation-induced flow around a droplet in different gases, Phys. Fluids 31 (9) (2019), 092109.
[40] T. Stoebe, Z. Lin, R.M. Hill, M.D. Ward, H.T. Davis, Surfactant-enhanced spreading, Langmuir 12 (2) (1996) 337–344.
[41] S. Rafaï, D. Sarker, V. Bergeron, J. Meunier, D. Bonn, Superspreading: aqueous surfactant drops spreading on hydrophobic surfaces, Langmuir 18 (26) (2002) 10486–10488.
[42] M.L. Sauleda, H.C.W. Chu, R.D. Tilton, S. Garoff, Surfactant driven Marangoni spreading in the presence of predeposited insoluble surfactant monolayers, Langmuir 37 (11) (2021) 3309–3320.
[43] M.D. Doganci, B.U. Sesli, H.Y. Erbil, Diffusion-controlled evaporation of sodium dodecyl sulfate solution drops placed on a hydrophobic substrate, J. Colloid Interface Sci. 362 (2011) 524–531.
[44] S. Semenov, A. Trybala, H. Agogo, N. Kovalchuk, F. Ortega, R.G. Rubio, V. M. Starov, M.G. Velarde, Evaporation of droplets of surfactant solutions, Langmuir 29 (32) (2013) 10028–10036.
[45] X. Zhong, F. Duan, Surfactant-adsorption-induced initial depinning behavior in evaporating water and nanofluid sessile droplets, Langmuir 31 (2015) 5291–5298.
[46] A. Marin, R. Liepelt, M. Rossi, C.J. Kähler, Surfactant-driven flow transitions in evaporating droplets, Soft Matter 12 (5) (2016) 1593–1600.
[47] W. Kwieciński, T. Segers, S. van der Werf, A. van Houselt, D. Lohse, H.J. W. Zandvliet, S. Kooij, Evaporation of dilute sodium dodecyl sulfate droplets on a hydrophobic substrate, Langmuir 35 (32) (2019) 10453–10460.
[48] J. Shi, L.S. Yang, C. Bain, Wetting and drying of aqueous droplets containing nonionic surfactant $C_nE_m$, Langmuir 37 (14) (2021) 4091–4101.
[49] Y.S. Yu, Substrate elastic deformation due to vertical component of liquid-vapor interfacial tension, Appl. Math. Mech. Eng. Ed. 33 (9) (2012) 1095–1114.
[50] J.L. Liu, X.Q. Feng, On elastocapillarity: a review, Acta Mech. Sin. 28 (4) (2012) 928–940.
[51] B. Andreotti, O. Bäumchen, F. Boulogne, K.E. Daniels, E.R. Dufresne, H. Perrin, Solid capillarity: When and how does surface tension deform soft solids? Soft Matter 12 (12) (2016), 2993-2296.
[52] M. van Gorcum, B. Andreotti, J.H. Snoeijer, S. Karpitschka, Dynamic solid surface tension causes droplet pinning and depinning, Phys. Rev. Lett. 121 (20) (2018), 208003.
[53] T. Huhtamäki, X.L. Tian, J.T. Korhonen, R.H.A. Ras, Surface-wetting characterization using contact-angle measurements, Nat. Protoc. 13 (7) (2018) 1521–1538.
[54] G.D. Miles, L. Shedlovsky, Minima in surface tension-concentration curves of solutions of sodium alcohol sulfates, J. Phys. Chem. 48 (1) (1944) 57–62.
[55] R. Khalladi, O. Benhabiles, F. Bentahar, N. Moulai-Mostefa, Surfactant remediation of diesel fuel pollted soil, J. Hazard. Mater. 164 (2–3) (2009) 1179–1184.
[56] L.Z. Wang, X.F. Huang, Q.Z. Yuan, L.Q. Chen, Y.S. Yu, Dilute sodium dodecyl sulfate droplets impact on micropillar-arrayed non-wetting surfaces, Phys. Fluids 33 (2021), 107103.

[57] V.M. Starov, S.R. Kosvintsev, M.G. Velarde, Spreading of surfactant solutions over hydrophobic substrates, J. Colloid Interface Sci. 227 (2000) 185–190.
[58] M. Duan, H. Wang, S.W. Fang, Y. Liang, Real-time monitoring the adsorption of sodium dodecyl sulfate on a hydrophobic surface using polarization interferometry, J. Colloid Interface Sci. 417 (2014) 285–292.
[59] T.A.H. Nguyen, A.V. Nguyen, Transient volume of evaporating sessile droplets: 2/3, 1/1, or another power law? Langmuir 30 (22) (2014) 6544–6547.